

## Local ultra-violet surface photovoltage spectroscopy of single thread dislocations in gallium nitrides by Kelvin probe force microscopy

Zhenghui Liu, Ke Xu, Yingmin Fan, Gengzhao Xu, Zengli Huang et al.

Citation: *Appl. Phys. Lett.* **101**, 252107 (2012); doi: 10.1063/1.4772538

View online: <http://dx.doi.org/10.1063/1.4772538>

View Table of Contents: <http://apl.aip.org/resource/1/APPLAB/v101/i25>

Published by the [American Institute of Physics](#).

---

### Related Articles

First-principles study of electronic structures and photocatalytic activity of low-Miller-index surfaces of ZnO  
*J. Appl. Phys.* **113**, 034903 (2013)

Temperature dependence of reversible switch-memory in electron field emission from ultrananocrystalline diamond  
*Appl. Phys. Lett.* **101**, 173116 (2012)

Investigation of the conduction in an implanted layer of protons in a potassium lithium tantalate niobate substrate  
*Appl. Phys. Lett.* **101**, 141111 (2012)

Transport properties of surface electrons in helium on a structured substrate  
*Low Temp. Phys.* **38**, 915 (2012)

Carrier doping to the organic Mott insulator by conjugating with tetrathiafulvalene  
*APL: Org. Electron. Photonics* **5**, 201 (2012)

---

### Additional information on *Appl. Phys. Lett.*

Journal Homepage: <http://apl.aip.org/>

Journal Information: [http://apl.aip.org/about/about\\_the\\_journal](http://apl.aip.org/about/about_the_journal)

Top downloads: [http://apl.aip.org/features/most\\_downloaded](http://apl.aip.org/features/most_downloaded)

Information for Authors: <http://apl.aip.org/authors>

## ADVERTISEMENT

**JANIS** Does your research require low temperatures? Contact Janis today.  
Our engineers will assist you in choosing the best system for your application.



10 mK to 800 K  
Cryocoolers  
Dilution Refrigerator Systems  
Micro-manipulated Probe Stations

LHe/LN<sub>2</sub> Cryostats  
Magnet Systems

[sales@janis.com](mailto:sales@janis.com) [www.janis.com](http://www.janis.com)  
Click to view our product web page.

## Local ultra-violet surface photovoltage spectroscopy of single thread dislocations in gallium nitrides by Kelvin probe force microscopy

Zhenghui Liu (刘争晖),<sup>1,2</sup> Ke Xu (徐科),<sup>1,2,a)</sup> Yingmin Fan (樊英民),<sup>1</sup>  
 Gengzhao Xu (徐耿钊),<sup>1</sup> Zengli Huang (黄增立),<sup>1</sup> Haijian Zhong (钟海帆),<sup>1</sup>  
 Jianfeng Wang (王建峰),<sup>1</sup> and Hui Yang (杨辉)<sup>2</sup>

<sup>1</sup>Platform for Characterization and Test, Suzhou Institute of Nano-tech and Nano-bionics, CAS, Suzhou 215123, People's Republic of China

<sup>2</sup>Key Laboratory of Nanodevices and Applications, Suzhou Institute of Nano-tech and Nano-bionics, CAS, Suzhou 215123, People's Republic of China

(Received 20 August 2012; accepted 30 November 2012; published online 19 December 2012)

The local carrier properties, including minority diffusion lengths and surface recombination velocities, were measured at single thread dislocations in GaN film by a combination of surface photovoltage spectroscopy and Kelvin probe force microscopy. The thread dislocations introduced by a nanoindentation were observed as V-pits, where the photovoltage was lower than that on plane surface under ultra-violet illumination. A model is proposed to fit the spatially resolved surface photovoltage spectroscopy curves. Compared with those on plane surface, the hole diffusion length is 90 nm shorter and the surface electron recombination velocity is 1.6 times higher at an individual thread dislocation. © 2012 American Institute of Physics. [<http://dx.doi.org/10.1063/1.4772538>]

Gallium nitride (GaN) is a promising material for its applications in optical and electronic devices. Carrier properties in GaN including minority diffusion lengths and surface recombination velocities are of significant importance in improving device performances. For instance, in Schottky or p-n junction photovoltaic detectors, due to a large absorption coefficient of GaN, carriers are generated close to the surface and recombine. A sufficiently long minority diffusion length and a suppression of surface recombination velocity are helpful in the realization of high sensitivity.<sup>1</sup> There are similar requirements for other GaN-based devices, including heterojunction bipolar transistors<sup>2</sup> and Schottky barrier or p-n diodes.<sup>3</sup> It is known that these carrier properties strongly depend on the density of thread dislocations, which is usually high for GaN films grown heteroepitaxially on non-native substrates such as sapphire and SiC.<sup>2-4</sup> Therefore, a better understanding of the dislocation structures and their influence on carrier properties is necessary. However, for most of the characterization methods, such as photoluminescence,<sup>5</sup> surface photovoltage (SPV),<sup>6</sup> and photocurrent<sup>7</sup> measurements, the spatial resolution of as-measured carrier properties is low, which makes it difficult to reveal the relationship between the experimental results and the local dislocation structures. Electron beam induced current (EBIC) method is capable of achieving the inhomogeneity of minority diffusion length along a depth gradient, but a p-n junction or a Schottky barrier has to be made at cross-section.<sup>8,9</sup> A simultaneous measurement of the topography, the local minority diffusion length, and the surface recombination velocity at a single thread dislocation is still needed.

In this letter, we demonstrate a non-destructive way to meet this goal with a combination of surface photovoltage spectroscopy (SPS) method and Kelvin probe force microscopy (KPFM). The contact potential difference (CPD) at

nanometer scale varying with the incident photon energy was measured with corresponding topography image. SPS responses at single thread dislocations near a nanoindentation on a GaN surface can be distinguished. A model to quantitatively analyze the minority diffusion length and the surface recombination velocity from the measured SPS spectra is proposed. There is a reduction of minority diffusion length by 90 nm and 1.6 times higher surface recombination velocity at dislocation positions compared with those measured in plane area.

Fig. 1(a) is the schematic diagram of our homemade experimental setup for local ultra-violet (UV) SPS tests. A Pt-coated tip (ACCESS-EFM, Appnano) was utilized to measure the CPD with KPFM method. The tetrahedral tip that protrudes from the very end of a cantilever made less shadow under the illumination of a beam of upright incident light. The KPFM measurements were performed in two-pass mode on an atomic force microscope (AFM) (NTEGRA SPECTRA, NT-MDT) under protection of nitrogen atmosphere. The topography was obtained in the first pass. Then in the second pass, the tip was lifted by 100 nm and follows the trace of topography. An AC voltage of 2.0 V was applied on the tip. A DC voltage was generated by a feedback loop to nullify the oscillation of the cantilever and was recorded as measured CPD.

The tunable monochromatic light was generated by a 450 W xenon lamp and a monochromator (IHR320, Horiba JY). A long pass filter of 324 nm is inserted to prevent the secondary scattering of the spectrometer. In our experiments, the slit width of the monochromator is 0.6 mm corresponding to 0.5 nm spectral resolution. The monolight was carried by a fiber to avoid the vibration of the AFM head. The output of fiber was aligned by a collimator and focused by an UV objective (50×, 0.55 N.A.) into a spot with a diameter of 20–25 μm. In literatures for local SPS measurements with illumination at visible range,<sup>10-12</sup> the output of fiber is

<sup>a)</sup>Electronic mail: kxu2006@sinano.ac.cn.

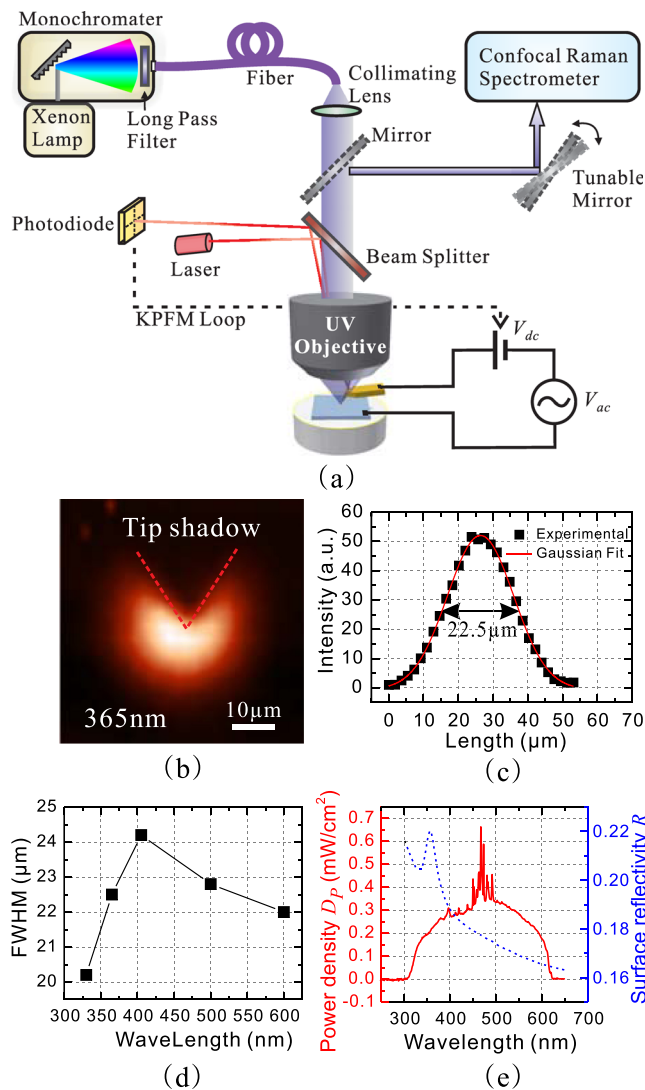


FIG. 1. (a) Experimental setup for local surface photovoltage measurements in UV spectral range. (b) The distribution of light intensity around the position where the AFM tip is located on a GaN surface. The red line indicates the tip shadow. (c) The profile of the light spot. (d) The diameter of the light spot versus wavelength. (e) The red curve is the power density of light  $D_P$  versus wavelength and the blue dashed curve is the surface reflectivity  $R$  of GaN versus wavelength calculated by FDTD method.

directly illuminated on the tip position with a large light spot at millimeter scale. With such configuration, the power density of light would be weaker at UV range than that at visible range because of the inhomogeneous output of Xenon lamp. Therefore, in our configuration, the UV objective was added to obtain higher power density for the enhancement of SPS response at nanometer scale. To measure the spot size, a

half-transparent mirror was inserted between the collimator and the objective. The light reflected by the mirror was collected by a confocal Raman spectrometer (HR800, Horiba JY). A piezo-driven mirror on the collection path can scan its angle in X/Y directions and make a confocal mapping of the light intensity around the spot. The results are shown in Fig. 1(b). The shadow of the projected tip and cantilever was marked by red lines, which can help the tip positioning at the center of the focused light spot. The intensity profile of the light spot is shown in Fig. 1(c) with a full width at half maximum (FWHM) of  $22.5 \mu\text{m}$  at  $365 \text{ nm}$  wavelength. In the spectral range from UV to visible, the change of the spot size caused by chromatic dispersion is shown in Fig. 1(d). The measured FWHM at  $330\text{--}650 \text{ nm}$  ranged from  $20$  to  $24.5 \mu\text{m}$ . As shown in Fig. 1(e), the power density of light versus wavelength was calculated by dividing the measured light power underneath the UV objective by the area of light spot. The local SPS was acquired by ramping the light wavelength from  $600$  to  $330 \text{ nm}$  with a fixed stepwise of  $1.0 \text{ nm}$ . At each wavelength, the tip was held at the same position until a steady CPD was measured.

The sample was a free-standing native n-type GaN grown by hydride vapor phase epitaxy (HVPE) method with a thickness of  $0.3 \text{ mm}$  (Suzhou Nanowin Co. Ltd., Suzhou, China). The dislocations density of as-grown crystal was extremely low ( $< 10^6 \text{ cm}^{-2}$ ). At the center of the scanned area shown in Fig. 2(a), a nanoindentation with a depth of about  $290 \text{ nm}$  is produced using a nanoindentation system (Nano Indenter G200, Agilent) with a Berkovich diamond tip following the same procedure in Ref. 13. The indentation introduces defects including point defects and thread dislocations.<sup>13</sup> At the top-left corner in Fig. 2(a), several V-pits associated with the termination of thread dislocations can be observed. The depth of the V-pit in the red circle marked with A is measured to be about  $1.0 \text{ nm}$  in the topography profile shown in Fig. 2(a). Fig. 2(b) is the CPD image of the same area in darkness condition. As shown in the CPD profile in Fig. 2(b), the same CPD values of about  $607 \text{ mV}$  are measured for the dislocation position A and the nearby plane position marked with B. However, under above-bandgap light excitation, lower CPD can be observed at the V-pit positions. Fig. 2(c) is the CPD image under illumination of monochromatic light with the wavelength of  $360 \text{ nm}$ . The V-pit positions show dark points in the image. As shown in the CPD profile in Fig. 2(c), the CPD at the plane position B is increased to  $776 \text{ mV}$  by a SPV value of  $168 \text{ mV}$ . The SPV at dislocation position A is  $155 \text{ mV}$ , which is  $13 \text{ mV}$  less than that at position B. For a quantitative analysis of the local carrier properties, the SPS  $V_L(\lambda)$  were measured at the

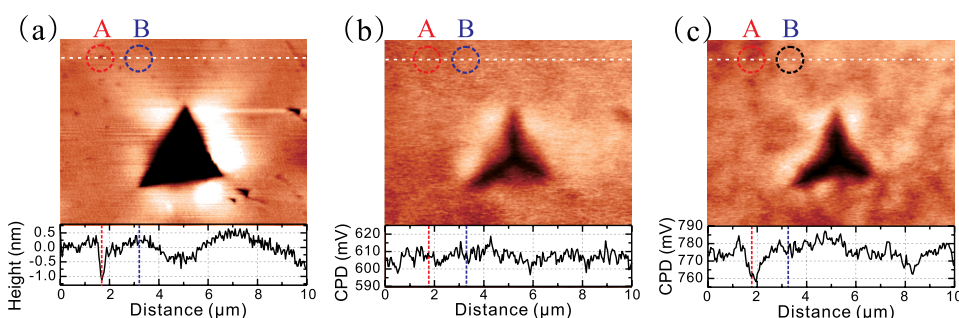


FIG. 2. (a) The topographic image around a nanoindentation with a scan area of  $10 \times 10 \mu\text{m}$ . A V-pit of thread dislocation is marked with A and a nearby plane position is marked with B. (b) and (c) are the CPD images of the same area acquired under dark condition and under UV illumination with wavelength of  $360 \text{ nm}$ , respectively. The curves in the images are the profiles along the white lines.

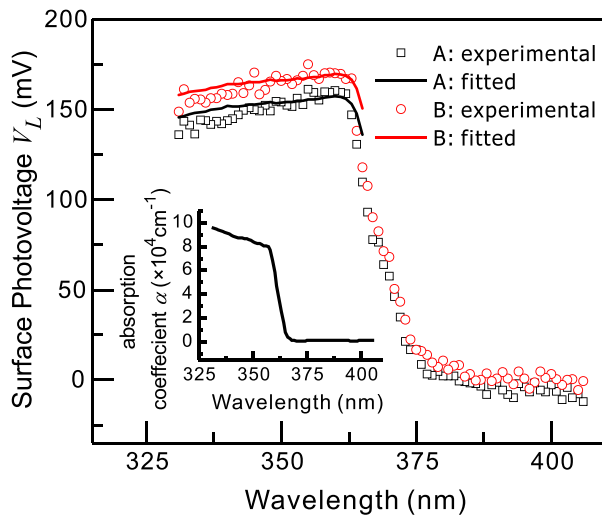


FIG. 3. The red circles and the black squares are local SPS  $V_L(\lambda)$  measured at the dislocation position A and the plane position B, respectively. The red and black lines are fitted SPS curves with Eq. (4). The inset is the absorption coefficient  $\alpha(\lambda)$  for GaN applied in fitting process.

dislocation position A and the plane position B, respectively, as shown in Fig. 3.

The calculation of the local minority diffusion length and the surface recombination velocity from the SPS data is as follows. The typical band diagram near the surface of n-type semiconductor is shown in Fig. 4(a). At the semiconductor surface, surface states are formed due to the disorder, dangling bonds, and adsorbents. The filling of surface states causes negative surface charges with density of  $n_s$ . The upward band bending is formed with a depletion region width  $W$ . The capture of bulk electrons by unoccupied surface states and the emission of electrons from occupied surface states into the bulk are described by the carriers flows:  $R_{bs}$  and  $R_{sb}$ . In the darkness, the flow of electron is in equilibrium:<sup>6</sup>

$$R_{bs} = R_{sb} = R_0 = s_n N_C \exp\left(-\frac{q\Phi_0}{kT}\right), \quad (1)$$

where  $s_n$  is the surface electron recombination velocity,  $N_C$  is the effective density of states in the conduction band,  $q$  is

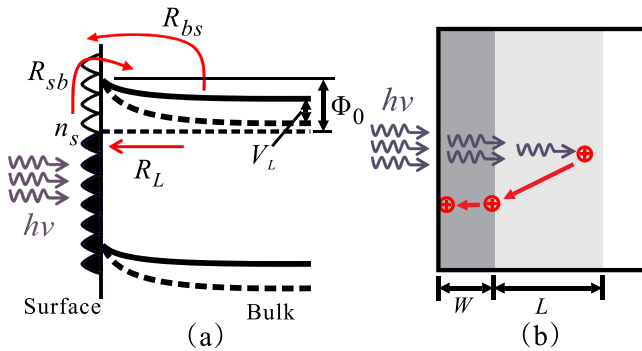


FIG. 4. (a) The band diagram at an n-type semiconductor surface in darkness (dashed line) and under illumination (solid line). (b) A schematic of the diffusion of photo-generated holes in bulk. Definitions of symbols:  $n_s$  is the surface charge density,  $R_{bs}$  is the electron flow from the bulk captured by unoccupied surface states,  $R_{sb}$  is the electron flow emitted from occupied surface state into the bulk,  $R_L$  is the photo-generated holes flow,  $\Phi_0$  is the distance between the surface Fermi level and the conduction band in darkness,  $V_L$  is the surface photovoltage,  $h\nu$  is the photon energy.

the electron charge, and  $\Phi_0$  is the distance between the surface Fermi level and the conduction band as shown in Fig. 4(a).

Under the illumination with a photon energy of  $h\nu$ , additional flow of carriers  $R_L$  is generated which changes the band bending by a SPV value  $V_L$ , as shown in Fig. 4(a). Considering that the density of surface states is of the order of  $10^{14} \text{ cm}^{-2}$  while the density of surface charge  $n_s$  is of the order of  $10^{12} \text{ cm}^{-2}$  for GaN, the distance between the surface Fermi level and the conduction band  $\Phi_0$  keeps almost unchanged and thus the rate  $R_{sb}$  of electrons emitted from the surface level is the same as that in darkness expressed by Eq. (1). However, the reduction of band bending makes the rate  $R_{bs}$  of bulk-to-surface electron flow change to

$$\begin{aligned} R_{bs} &= s_n N_C \exp\left(-\frac{q\Phi_0 - qV_L}{kT}\right) \\ &= R_0 \exp\left(\frac{qV_L}{kT}\right). \end{aligned} \quad (2)$$

In the case of above-bandgap excitation, photo-generated flow  $R_L$  mainly contributed by the bulk-to-surface flow of light-induced holes due to the separation of electron-hole pairs. As shown in Fig. 4(b), the absorption of light inside the bulk creates electro-hole pairs. On average, minority carriers (holes in the n-type semiconductor) created in the regions within a diffusion length of  $L$  live long enough to diffuse to the depletion region. These holes are subsequently swept to the surface along with the holes generated within the depletion region. Then, photo-generated flow of holes  $R_L$  is the light fluxes (photons per square centimeter per second) absorbed within a depth of  $(W+L)$  from the surface.<sup>14</sup> In our experiments, the samples are illuminated from the front side. The light fluxes  $P_0$ , therefore, decrease inside the bulk as  $\exp(-\alpha x)$ , where  $\alpha$  is the absorption coefficient and  $x=0$  at the surface. So,  $R_L$  can be calculated as

$$\begin{aligned} R_L &= \int_0^{W+L} \alpha P_0 e^{-\alpha x} dx \\ &= P_0 (1 - e^{-\alpha(W+L)}). \end{aligned} \quad (3)$$

Under continuous illumination, the net flow of electron to the surface is equal to the flow of photo-generated hole to the surface, i.e.,  $R_{bs} - R_{sb} = R_L$  in the steady-state condition. After substitution for  $R_{bs}$ ,  $R_{sb}$ , and  $R_L$  using Eqs. (1), (2), and (3), respectively, we get equation

$$(e^{qV_L/kT} - 1)/P_0 = (1 - e^{-\alpha(W+L)})/R_0. \quad (4)$$

Noting that  $V_L$ ,  $\alpha$ , and  $P_0$  are functions of the wavelength  $\lambda$ , parameters  $(W+L)$  and  $R_0$  can be fitted out with Eq. (4) if  $V_L(\lambda)$ ,  $\alpha(\lambda)$  and  $P_0(\lambda)$  are known. It should be noted that the commonly used equation for surface photovoltage  $V_L$  in single crystal silicon is not appropriate for the case of GaN. Assuming  $L \gg W$  and  $\alpha L \ll 1$ , the expression  $e^{-\alpha(W+L)}$  becomes  $1/(1 + \alpha L)$ . Then Eq. (4) can fall back to the commonly used form of SPV:<sup>15</sup>  $e^{qV_L/kT} - 1 = C\alpha L/(\alpha L + 1)$ , where  $C$  is a constant. However, these assumptions do not hold for the case of GaN with  $\alpha \sim 10^5 \text{ cm}^{-1}$ ,  $W \sim 0.1-0.3 \mu\text{m}$ , and  $L \sim 0.1-1 \mu\text{m}$ .

The SPS data with above-bandgap excitation ( $\lambda \geq 363$  nm) were fitted with Eq. (4), as shown in Fig. 3. The absorption coefficients  $\alpha(\lambda)$  for GaN applied in the fitting process were measured with ellipsometer and are shown in the inset of Fig. 3. The light flux  $P_0(\lambda)$  was calculated from the power density  $D_P(\lambda)$  shown in Fig. 1(e) with the expression  $P_0(\lambda) = D_P(\lambda)(1 - R(\lambda))/h\nu$ , where  $R$  is the surface reflectivity of GaN. It should be noted that the local reflectivity  $R$  may change due to the different topography. 3D finite difference time domain (FDTD) simulations (Lumerical Solution)<sup>16</sup> were performed to calculate  $R$  for the plane surface and the V-pit structure around the thread dislocation, respectively. The calculated result for the plane surface is shown in Fig. 1(e). The diameter and depth of the simulated V-pit structure are 330 nm and 1 nm, respectively, as shown in the profile in Fig. 2(a). The differences of  $R$  between the plane surface and the V-pit structure are not more than  $2 \times 10^{-4}$ , which can be neglected. Then the parameters  $(W + L)$  and  $R_0$  are fitted to be  $0.64 \mu\text{m}$  and  $7.1 \times 10^{11} \text{cm}^{-2}\text{s}^{-1}$  for dislocation position A, and  $0.73 \mu\text{m}$  and  $4.5 \times 10^{11} \text{cm}^{-2}\text{s}^{-1}$  for plane position B. The fitted curves of SPS are shown in Fig. 3 with the red and black line. The order of values  $(W + L)$  matches the order of the minority diffusion lengths reported in literatures for HVPE-grown GaN measured by EBIC method.<sup>8,9</sup> The reduced value of  $(W + L)$  at the dislocation position A means shorter minority diffusion lengths at threading dislocations, which act as non-radiative recombination centers for holes, resulting in a reduced lifetime. From the fitted value of  $R_0$ , the surface recombination velocity  $s_n$  can be calculated with Eq. (1). The value of  $\Phi_0$  was obtained with the equation:<sup>17</sup>  $\Phi_0 = \Phi_{tip} - \chi - V_{dark} \approx 0.9$  V, where  $\Phi_{tip}$  is the work function of the Pt-coated tip (5.6 V),  $\chi$  is the electron affinity of GaN (4.1 V), and  $V_{dark}$  is the CPD measured in darkness (0.607 V). The effective density of states in the conduction band of GaN  $N_C$  is  $2.5 \times 10^{18} \text{cm}^{-3}$ .<sup>6</sup> Then, the surface recombination velocities for the dislocation position A and the plane position B are  $2.9 \times 10^8 \text{cm/s}$  and  $1.8 \times 10^8 \text{cm/s}$ , respectively. It should be noted that the value of  $s_n$  is very sensitive to the value of  $\Phi_0$ . For instance, the uncertainty of  $\Phi_0$  with the value of  $0.9 \pm 0.1$  V makes  $s_n$  change by a factor of about  $10^4$ . Therefore, the above calculations do not allow us to precisely determine the absolute value of  $s_n$ . However, the inhomogeneous of  $s_n$  with a value about 1.6 times larger at threading dislocations is credible with our local SPS method.

In conclusion, a combination of UV SPS and KPFM techniques has been introduced to measure the carrier properties at single thread dislocations in GaN film at nanometer scale. The thread dislocations were introduced by a nanoin-

dentation on a HVPE-grown GaN sample. Under UV illumination, a lower surface photovoltage by about 13 mV was observed at these dislocation positions compared with that obtained in plane area. By fitting the measured SPS curves with a model proposed for above-bandgap excitation, the information about minority diffusion lengths and surface recombination velocities can be quantitatively analyzed. The hole diffusion length at the thread dislocation is lower than that in plane area by a value of about 90 nm, while the surface recombination velocity at the thread dislocation is about 1.6 times larger than that in plane area. The results show that the SPS measurement with KPFM method is an effective way to estimate the local optoelectronic properties of dislocation structures in GaN films.

This work was partly supported by the NSFC (10904107), the Instrument Developing Project, CAS (YZ200939, YG2011071), MOST of China (2010DFA22770, 2011AA03A103, 2011DFR50390), and the NBRP (973 program) of China (2012CB619305).

<sup>1</sup>L. Chernyak, A. Osinsky, and A. Schulte, *Solid-State Electron.* **45**, 1687 (2001).

<sup>2</sup>Z. Lochner, H. J. Kim, Y.-C. Lee, Y. Zhang, S. Choi, S.-C. Shen, P. D. Yoder, J.-H. Ryou, and R. D. Dupuis, *Appl. Phys. Lett.* **99**, 193501 (2011).

<sup>3</sup>K. Mochizuki, K. Nomoto, Y. Hatakeyama, H. Katayose, T. Mishima, N. Kaneda, T. Tsuchiya, A. Terano, T. Ishigaki, T. Tsuchiya, R. Tsuchiya, and T. Nakamura, *IEEE Trans. Electron Devices* **59**, 1091 (2012).

<sup>4</sup>G. Moldovan, P. Kazemian, P. R. Edwards, V. K. Ong, O. Kurniawan, and C. J. Humphreys, *Ultramicroscopy* **107**, 382 (2007).

<sup>5</sup>P. Scajev, K. Jarasiunas, S. Okur, U. Oezguer, and H. Morkoc, *J. Appl. Phys.* **111**, 023702 (2012).

<sup>6</sup>M. A. Reshchikov, M. Foussekis, and A. A. Baski, *J. Appl. Phys.* **107**, 113535 (2010).

<sup>7</sup>D. Wee, G. Parish, and B. Nener, *J. Appl. Phys.* **111**, 074503 (2012).

<sup>8</sup>L. Chernyak, A. Osinsky, G. Nootz, A. Schulte, J. Jasinski, M. Benamara, Z. Liliental-Weber, D. C. Look, and R. J. Molnar, *Appl. Phys. Lett.* **77**, 2695 (2000).

<sup>9</sup>A. Cavallini, L. Polenta, and A. Castaldini, *Microelectron. Reliab.* **50**, 1398 (2010).

<sup>10</sup>S. Saraf, R. Shikler, J. Yang, and Y. Rosenwaks, *Appl. Phys. Lett.* **80**, 2586 (2002).

<sup>11</sup>L. Malikova, T. Holden, M. N. Perez-Paz, M. Muñoz, and M. C. Tamargo, *Appl. Phys. Lett.* **94**, 102109 (2009).

<sup>12</sup>F. Streicher, S. Sadewasser, and M. C. Lux-Steiner, *Rev. Sci. Instrum.* **80**, 013907 (2009).

<sup>13</sup>J. Huang, K. Xu, X. J. Gong, J. F. Wang, Y. M. Fan, J. Q. Liu, X. H. Zeng, G. Q. Ren, T. F. Zhou, and H. Yang, *Appl. Phys. Lett.* **98**, 221906 (2011).

<sup>14</sup>R. F. Pierret, *Semiconductor Device Fundamentals* (Addison-Wesley, 1996).

<sup>15</sup>D. K. Schroder, *Meas. Sci. Technol.* **12**, R16 (2001).

<sup>16</sup>E. Bisaiillon, D. Tan, B. Faraji, A. Kirk, L. Chrowstowski, and D. V. Plant, *Opt. Express* **14**, 2573 (2006).

<sup>17</sup>S. Barbet, R. Aubry, M. di Forte-Poisson, J. Jacquet, D. Deresmes, T. Melin, and D. Theron, *Appl. Phys. Lett.* **93**, 212107 (2008).